A | R | J
Amrit Research Journal December 2025, Vol. 6, Issue 1, 82-90
ISSN: 2738-9553
RESEARCH ARTICLE

Study the Structural, Dynamical, Electronic, and Magnetic Properties of $CoSb_3$ Skutterudite Material: First-Principles Approach

Sukrit Kumar Yadhav[1], Arun Devkota[1], Ganesh Paudel[1], Om Shree Rijal[1], Hari Krishna Neupane[1*], Rajendra Parajuli[1]
[1]Amrit Campus, Institute of Science and Technology, Tribhuvan University, Kathmandu Nepal
[*]E-mail: hari.neupane@ac.tu.edu.np

(Received: November 3, 2025, Received in revised form: November 20, 2025, Accepted: December 1, 2025, Available online: December 19, 2025)

DOI: https://doi.org/10.3126/arj.v6i1.87535

Highlights

- Investigated structural, dynamical, electronic, and magnetic properties of $CoSb_3$ skutterudites compound using DFT method through the VASP software
- $CoSb_3$ is a structurally stable which is confirmed by the estimated values of its bond length, formation and cohesive energies
- Dynamical stability confirmed by phonon band structure showing no imaginary frequency
- Metallic and magnetic behavior are observed through the analysis of its band structure, DOS and PDOS plots

Abstract

Skutterudite compounds have potential applications in optoelectronic, thermoelectric, and spintronic devices. In this work, we have explored the physical properties of the $CoSb_3$ skutterudite compound using the density functional theory (DFT) method with the GGA: PBE+U functional implemented in the VASP computational package. The structural properties of $CoSb_3$ have been investigated by optimizing its lattice parameters and bond lengths, as well as estimating its formation and cohesive energies. The results indicate that the compound is structurally stable. The dynamical properties of $CoSb_3$ were analyzed based on the obtained phonon dispersion curves. The absence of negative frequency modes at all high-symmetry points confirms that the material is dynamically stable. The electronic and magnetic properties were determined through the analysis of the band structure, density of states (DOS), and partial density of states (PDOS) plots. From the band structure and DOS results, $CoSb_3$ exhibits metallic behavior, as band states are observed around the Fermi energy level. For the magnetic properties, the DOS and PDOS analyses reveal that the compound possesses a finite magnetic moment, indicating that $CoSb_3$ is magnetic in nature. The observed magnetic moment arises from the dominant distribution of down-spin electronic states in the atomic orbitals of the constituent elements.

Keywords: *band, DFT, dynamical, electronic, magnetic, spin states*

Introduction

Skutterudite materials have been extensively investigated because of their exceptional and tunable thermoelectric, electronic, and magnetic properties (Rogl & Rogl, 2019; Li et al., 2017). These compounds are therefore highly promising for energy conversion and spintronic applications (Rogl & Rogl, 2019; Li et al., 2017). Among them, cobalt antimonide ($CoSb_3$) is a well-known

[*]Corresponding author

representative of this family. It has the general formula MX_3 where M = transition metal, X = Pnictogen (Rogl & Rogl, 2019). $CoSb_3$ crystallizes in a body-centered cubic structure (space group Im-3, No. 204), consisting of corner-sharing $CoSb_6$ octahedra and Sb_4 rings that form large voids in the lattice. These voids can be filled by foreign atoms, giving rise to filled skutterudites with significantly reduced lattice thermal conductivity and enhanced thermoelectric efficiency (Li et al., 2017). Understanding the intrinsic physical properties of the unfilled $CoSb_3$ framework is therefore essential for optimizing the performance of its filled derivatives (Li et al., 2017). Despite its technological importance, accurately describing $CoSb_3$ theoretically remains challenging. Density functional theory (DFT) method of calculations within the generalized gradient approximation (GGA) often underestimate the band gap or even predict a metallic and magnetic ground state (Li et al., 2017; Khan et al., 2015). However, experiments have confirmed that $CoSb_3$ is a narrow-gap semiconductor with a band gap of about 0.2 eV and exhibits diamagnetic behavior (Khan et al., 2015). Similarly, $FeSb_2$, another transition-metal antimonide, is found to be metallic under GGA but corrected to a semiconducting state by hybrid or GGA+U treatments (Malki et al., 2022). This inconsistency primarily arises from the inadequate treatment of localized Co-3d electrons within the conventional GGA method. The GGA+U approach effectively improves the description of electron correlation and provides more accurate electronic and magnetic properties.

Apart from electronic properties, it is crucial to understand the structural and dynamical stability of $CoSb_3$. The phonon dispersion provides important insights into lattice vibrations and dynamically stability. The absence of imaginary frequencies indicates that the optimized structure is dynamically stable (Kong, 2011). The interaction between Co-3d and Sb-5p orbitals, in addition to determining the nature of bonding and band dispersion, also plays a key role in possible spin polarization and weak magnetic behavior, as observed in some calculations (Rana & Barman, 2013). In this context, the present work performs the investigation of physical properties specially focus on structural, dynamical, electronic and magnetic properties of $CoSb_3$ using the first-principles calculations through GGA: PBE+U exchange-correlation functional implemented the Vienna ab initio Simulation Package (VASP) computational software (Hafner, 2008; Hafner & Kresse, 1997). The structural properties are optimized and relaxed to determine the equilibrium lattice parameters and bond lengths. The phonon band structure is analyzed to confirm dynamic stability. The electronic properties are examined through band structure and density of states (DOS) analyses, while the magnetic characteristics are investigated using DOS and partial DOS (PDOS) calculations which explore orbital-resolved contributions. This comprehensive investigation aims to provide microscopic insight into the intrinsic structure, bonding, and electronic interactions in $CoSb_3$, thereby contributing to the theoretical foundation for its optimization in thermoelectric and spintronic applications.

Methodology

In this work, we have systematically investigated the structural, electronic, magnetic, and dynamical properties of $CoSb_3$ skutterudite material using density functional theory (DFT) methods (Hohenberg & Kohn, 1964) as implemented in the Vienna ab initio Simulation Package (VASP) (Hafner & Kresse, 1997). The electronic exchange-correlation potential was treated within the generalized gradient approximation (GGA) (Kohn & Sham, 1965) and its extension, the PBE+U functional (Verma & Truhlar, 2016). Hubbard U values of 3 eV for the p-orbitals and 5 eV for the d-orbitals of the constituent atoms were employed. These parameters were selected based on previous computational studies demonstrating their effectiveness in correcting self-interaction errors and capturing the localized nature of Co-d and Sb-p states (Concoction & De Gironcoli, 2005; Yu et al., 2020). A plane-wave kinetic energy cutoff of 520 eV and a convergence threshold of 10^{-7} eV were used to ensure high computational accuracy. The equilibrium lattice parameters and atomic configurations were obtained by minimizing both the cell pressure and atomic forces until the Hellmann-Feynman force (Ventra & Pantelides, 2000) on each atom was reduced below 0.01 eV/Å. The electronic and magnetic properties of the optimized $CoSb_3$ structure were analyzed through band structure, density of states (DOS), and partial density of states (PDOS) calculations. For the electronic band structure, a (12×12×12) Monkhorst–Pack k-point grid (Monkhorst & Pack, 1976) was employed, while a denser (24×24×24) grid was used for DOS and PDOS calculations to obtain smoother and more resolved spectral features. These analyses enabled a detailed understanding of the contributions of different atomic orbitals to the valence and conduction bands and provided insights into the material's electronic transitions and magnetic polarization. The dynamical stability of $CoSb_3$ was evaluated using density functional perturbation theory (DFPT) (Togo & Tanaka, 2015) by calculating its phonon dispersion relations.

Results and Discussion

In this section, the key findings of the present study are presented, and compared these findings with the similar kinds of the available reported works.

Structural Properties

Cobalt antimonide ($CoSb_3$) crystallizes in a cubic skutterudite structure with space group Im-3 (No. 204). The structure can be described as a binary skutterudite framework derived from the prototype compound $CoAs_3$ (Rogl & Rogl, 2019; Li et al., 2017). In this structure, each cobalt atom occupies the 8c Wyckoff position (¼, ¼, ¼), while antimony atoms occupy the 24g positions (0, *y*, *z*), where *y* and *z* are internal positional parameters that determine the degree of distortion of the Sb_4 rings. The unit cell contains 32 atoms, with each Co atom octahedrally coordinated by six Sb atoms, forming a slightly distorted $CoSb_6$ octahedron. The Sb atoms form four-membered (Sb_4) rings that create large voids within the structure. These voids are essential for the formation of filled skutterudite derivatives, which are widely used in thermoelectric applications (Rogl & Rogl, 2019). Figure-1 shows the relaxed unit cell in the ab-plane, where Co atoms are represented by red spheres and Sb atoms by blue spheres.

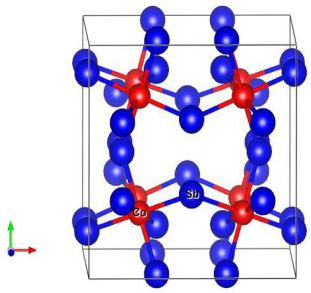

Fig. 1. (Colour online) Optimized and relaxed cubic structure of $CoSb_3$ unit cell. Red spheres represent Co atoms and blue spheres represent Sb atoms.

The estimated values of lattice parameters and bond lengths are summarized in Table-1. The values before and after relaxation are presented in reference to those reported in previous studies. The lattice parameters (a = b = c) and bond lengths (Co-Sb, Sb-Sb, and Co-Co) increased after relaxation. The lattice parameter before relaxation was 9.05 Å, which increased to 9.18 Å after relaxation-values consistent with previous reports of approximately 9.03 Å (Savchuk et al., 2002). The Co-Sb, Sb-Sb, and Co-Co bond lengths before relaxation were 2.53 Å, 3.71 Å, and 4.56 Å, respectively. After relaxation, these bond lengths increased to 2.55 Å, 3.73 Å, and 4.57 Å, respectively. The first two bond lengths are in good agreement with values reported in earlier studies (Caillat et al., 1996; Rodrigues et al., 2022).

Table 1. Lattice parameters (a = b = c) and bond lengths between (Co-Sb, Sb-Sb and Co-Co) atoms in the $CoSb_3$ structure are obtained from before and after relaxed calculations, and they are compared with the reported values.

	Estimated value	**Reported Value**	**Estimated value**	**Reported Value**	**Estimated value**	**Reported Value**	**Estimated value**	**Reported Value**
	a = b = c (Å)		Co-Sb (Å)		Sb-Sb (Å)		Co-Co (Å)	
Before relaxing	9.05	-	2.53	-	3.71	-	4.56	-
After relaxing	9.18	9.03 [a]	2.55	2.54 [b]	3.73	3.73 [c]	4.57	-

[a]:(Savchuk et al., 2002); [b]:(Caillat et al., 1996); [c]: (Rodrigues et al., 2022)

Moreover, we examined the chemical stability of the $CoSb_3$ material by calculating its formation energy (E_{form}) and cohesive energy (E_{coh}). A lower value of formation energy indicates higher material stability, whereas a greater value of cohesive energy signifies stronger atomic bonding, which also contributes to overall structural stability. The formation of energy and counterpoise-corrected cohesive energy were calculated using equations (1) and (2), respectively (Atkins et al., 2023; Hammerschmidt et al., 2013);

$$E_{formation} = E_{total}(CoSb_3) - [E_{total}(Co) + 3E_{total}(Sb)] \quad \ldots (1)$$

$$E_{Cohehive} = E_{CoSb3} - E_{Co} - 3E_{Sb} \quad \ldots (2)$$

The calculated values of formation energy and cohesive energy for $CoSb_3$ within the PBE+U functional are found to be -43 meV and -17.98 eV, respectively. These values are in close agreement with previously reported results obtained using different functionals of similar materials (Hammerschmidt et al., 2013; Park & Kim, 2010). Based on the calculated bond lengths, lattice parameters, formation energy, and cohesive energy, it can be concluded that $CoSb_3$ is structurally stable.

Phonon Band Structure

To investigate the dynamical stability of $CoSb_3$, the phonon band structure was studied. Figure-2 illustrates how the frequencies (or energies) of quantized lattice vibrations (phonons) vary along high-symmetric paths in the first Brillouin zone. The phonon frequencies are shown along the *y*-axis, while the high-symmetry points are plotted along the *x*-axis. Real and positive phonon frequencies occur when a restoring force acts to return displaced atoms to their equilibrium positions, indicating dynamical stability of the material (Pokharel et al., 2025; Yadav et al., 2025). In contrast, imaginary phonon frequencies arise when no restoring force exists, leading to dynamical instability (Kong, 2011).

In Figure-2, the horizontal blue dashed line at zero frequency separates the positive-frequency region from the imaginary-frequency region. The low-frequency acoustic phonons are represented in green, with two transverse branches and one longitudinal branch. The high-frequency optical phonons are shown in red, comprising a total of forty-five optical branches. All acoustic and optical phonon branches exhibit real and positive frequencies, as all the curves lie above the zero-frequency line. These results confirm that $CoSb_3$ is dynamically stable.

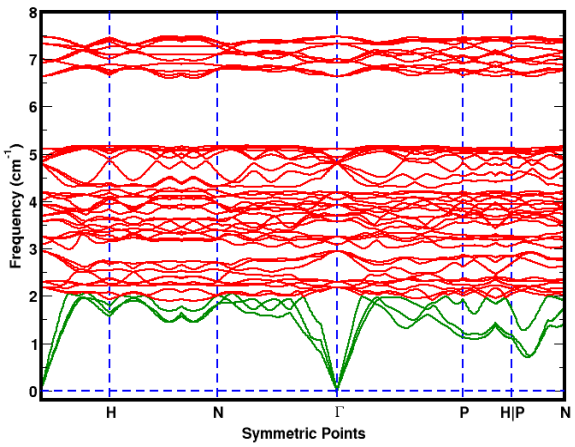

Fig. 2. (Colour online) Phonon band structure of $CoSb_3$ compound which was obtained by employing GGA: PBE+U functional in the DFT method of calculations. the vertical dot lines touches the highly symmetric points in the irreducible Brillion zone.

Furthermore, the optical modes can be seen to cluster into four distinct frequency bands. The possible reasons for this band separation are the mass difference between Co (58.933 u) and Sb (121.760 u), variations in bond strengths, and the localization of Co vibrations (cage effect). Phonon frequencies are inversely related to atomic masses; thus, the lower frequencies originate from the heavier Sb atoms, while the higher-frequency phonons are associated with the lighter Co atoms. The Co atoms, located at the centers of Sb_6 octahedral cages, form strong covalent bonds with Sb atoms, whereas Sb-Sb interactions are comparatively weaker (Rogl & Rogl, 2019). Consequently, vibrations involving Co-Sb stretching require higher energy and therefore appear at higher frequencies, while Sb-Sb bending vibrations occur at lower frequencies. In addition, the large band gap between the two optical groups arises from the rattling motion of Co atoms within the Sb_6 cages, which is characteristic of structural rigidity and phonon localization-features that are crucial for the thermoelectric performance of $CoSb_3$ (Rogl & Rogl, 2019).

Electronic Band Structure

Determining the electrical nature of a material is essential for exploring its potential device applications (Neupane et al., 2025; Paudel et al., 2023) For this purpose, the band structure and density of states (DOS) of $CoSb_3$ were studied. Figure-3 shows the band and DOS plot of $CoSb_3$ material within the GGA: PBE+U approximation. The left panel displays the variation of electron

energy (with the Fermi energy shifted to 0 eV) along high-symmetry directions in the Brillouin zone. The blue dashed horizontal line at 0 eV separates the upper conduction band from the lower valence band is called Fermi energy level. The right panel shows the total DOS (TDOS, in black) and the contributions from Co (in magenta) and Sb (in green) atoms. The DOS provides information on how densely electronic states are distributed at each energy level. High DOS indicates a greater availability of states, allowing electrons to occupy or transition more easily, whereas low DOS suggests fewer available states and reduced electronic activity at those energy levels (Neupane et al., 2025; Paudel et al., 2023).

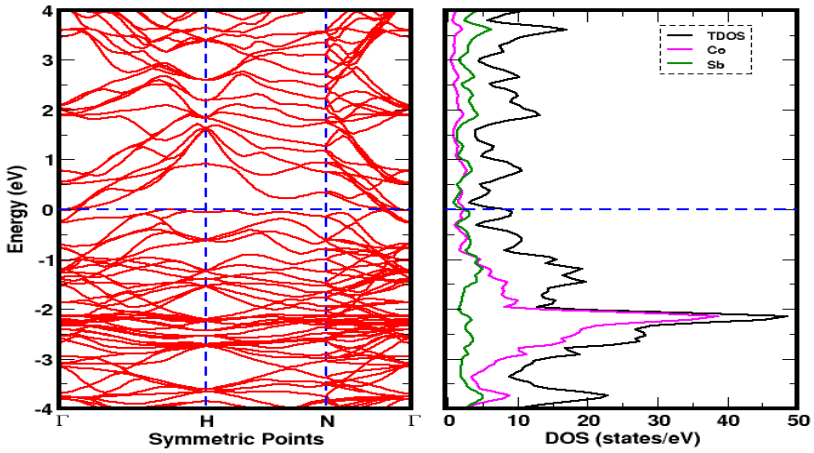

Fig. 3. (Colour online) Band and DOS plot of $CoSb_3$ compound which are obtained by employing GGA: PBE+U functional in DFT calculations through VASP computational software. The horizontal dotted line represents the Fermi energy level which separates the valence band and conduction band while vertical dotted lines denote the symmetric points in the irreducible Brillion zone of crystal structure.

Figure-3 shows no distinct band gap, with finite states present at the Fermi level. This suggests a metallic characteristic of the material. This result is similar with the experimental results of others skutterudite materials (Khan et al., 2015). Similar behavior has also been reported in previous DFT studies of other binary skutterudite materials, where the semiconducting gap was recovered after applying computationally intensive methods such as Green's Function (GW) or the regular and non-regular Tran-Blaha modified Becke-Johnson (TB-mBJ) approaches. Therefore, the current results reflect the exchange–correlation treatment rather than only a fundamental change in the electronic nature of $CoSb_3$ (Khan et al., 2015).

Furthermore, both Co and Sb contribute approximately equally to the DOS near the Fermi energy. The states in the conduction band are relatively sparser than those in the valence band. This asymmetry indicates that the valence band is more dispersive and composed of hybridized Co-3d and Sb-5p orbitals, whereas the conduction band is dominated primarily by less dispersive Co-3d, Sb-5p states. The asymmetric DOS distribution suggests that p-type carriers are more easily generated than n-type carriers, which is consistent with the experimentally observed thermoelectric behavior of $CoSb_3$ (Li & Mingo, 2014).

Magnetic Properties

The magnetic properties of a material need to be studied to identify magnetic ordering, predict potential spintronic applications, and guide material engineering (Neupane et al., 2025; Neupane et al., 2025). In the present work, the magnetic properties of $CoSb_3$ were investigated by calculating the spin-polarized density of states (DOS) and partial density of states (PDOS). Spin-polarized DOS separates spin-up and spin-down electron densities, revealing the net magnetic moment per atom or per unit cell (Paudel et al., 2023; Rijal et al., 2025). Similarly, PDOS decomposes the DOS into atomic and orbital contributions, allowing a detailed analysis of the magnetic nature of the material and identification of the orbitals that form the valence and conduction bands (Bardeen, 1937). The electronic configuration of Co is [Ar] $4s^2$ $3d^7$, and that of Sb is [Kr] $4d^{10}$ $5s^2$ $5p^3$. The contributions of the valence and penultimate orbit electrons are discussed below.

In Figure-4, the DOS of $CoSb_3$ calculated using the GGA: PBE+U approximation is shown. The DOS (in states/eV) is plotted along the *y*-axis, while the Fermi-shifted energy levels (in eV) are plotted along the *x*-axis. The contributions of Co and Sb to the DOS are indicated in red and green lines, respectively. The vertical blue dashed line at the Fermi energy level (0 eV) separates the valence band on the left from the conduction band on the right. Similarly, the horizontal blue dashed line at 0 states/eV separates the upper spin-up channel from the lower spin-down channel.

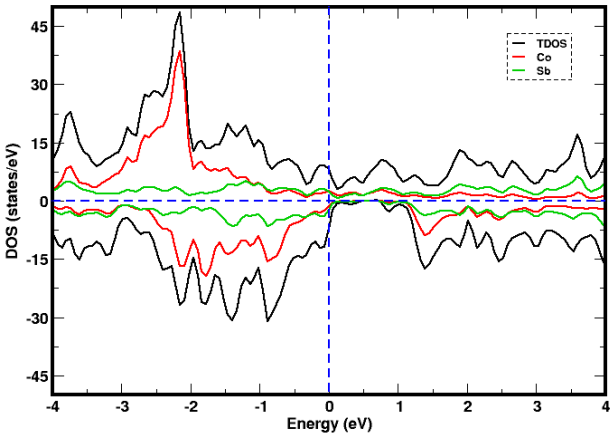

Fig. 4. (Colour online) Density of states (DOS) plot of $CoSb_3$ material where horizontal dotted line distinguishes the distributed spin-up and spin-down states while vertically dotted line indicates the fermi energy level which separates the valence and conduction bands. The region below the 0 eV point is called valence band and above the 0 eV is called conduction band.

In Figure-4, an asymmetrical distribution of the DOS can be observed between the spin-up and spin-down channels. The DOS contribution from Co spin-up states is greater than that from spin-down states. In contrast, the DOS contributions from Sb spin-up and spin-down states are nearly symmetrical, with a slightly higher contribution from spin-up states. This asymmetry in the DOS indicates a difference in the magnetic moments contributed by spin-up and spin-down electrons, resulting in a net magnetic moment and suggesting magnetic behavior of $CoSb_3$ within the GGA: PBE+U approximation. This result is aggregable with the reported work of other skutterudite materials (Lue et al., 2007).

Figure-5 shows the partial density of states plots where total DOS (TDOS) of $CoSb_3$ compound is represented by top graph, and the sub-orbital contributions of Co atoms in $CoSb_3$ were shown by middle graph, and contribution of Sb atoms in $CoSb_3$ compound are shown in the bottom graph. The DOS is plotted along the *y*-axis, and energy levels are plotted along the *x*-axis. The horizontal blue dashed line separates the upper spin-up channel from the lower spin-down channel, while the vertical blue dashed line marks the boundary between the valence band (left) and the conduction band (right). All three graphs are asymmetrical about the horizontal line. In the case of Co, the area under the spin-up curves above the horizontal line is greater than the area of the spin-down curves below it, indicating a higher number of spin-up states than spin-down states. A similar but opposite trend is observed for Sb, where the spin-down states are relatively numerous than the spin-up states. This difference between spin-up and spin-down states results in a net magnetic moment, suggesting a magnetic character for $CoSb_3$ for GGA: PBE+U functional.

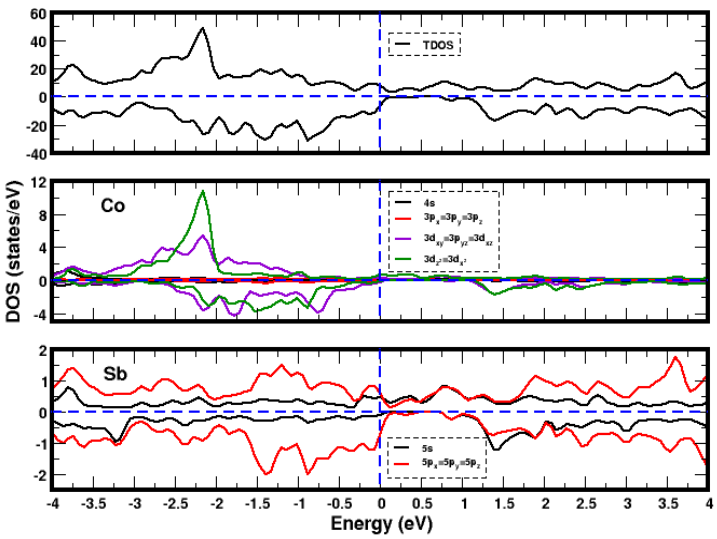

Fig. 5. (Colour online) Partial density of states plots of $CoSb_3$. In top graph, we determined the magnetic moment contributed by total spin-up states and total spin-down states. Middle and bottom plots are obtained by the asymmetric distributed spin-up and spin-down electronic states of Co and Sb atoms respectively in $CoSb_3$ compound.

Furthermore, it can be observed that the conduction band is dominated by the 3d orbitals of Co atoms, whereas the valence band is contributed approximately equally by both Co and Sb orbitals. Among the Co-3d sub-orbitals, $3dz^2$ and $3d_{x^2-y^2}$ dominate the conduction band, followed by the $3d_{xy}$, $3d_{yz}$, and $3d_{xz}$ sub-orbitals. All three p sub-orbitals (i.e., p_x, p_y, and p_z) of Co atoms contribute equally to their respective spin-up and spin-down channels. A similar pattern is observed for Sb atoms as well. The equal DOS contributions from the respective sub-orbitals indicate identical intensity and energy distribution, suggesting that these states remain degenerate under the local crystal field. This degeneracy arises from the nearly octahedral coordination of Co atoms surrounding Sb atoms in the skutterudite lattice (Lue et al., 2007). To study the orbital contributions in detail, the magnetic moment contributions from each sub-orbital of both Co and Sb were calculated and are presented in Table-2. For Co atoms, the spin-up and spin-down contributions are 1.272 μ_B/cell and -2.513 μ_B/cell, respectively, resulting in a net magnetic moment of -1.241 μ_B/cell. Similarly, for Sb atoms, the spin-up and spin-down contributions are 1.126 μ_B/cell and -1.103 μ_B/cell, respectively, yielding a net magnetic moment of 0.023 μ_B/cell. The total net magnetic moment of $CoSb_3$ is therefore -1.218 μ_B/cell. The negative value of magnetic moment indicates that there was dominant contribution of magnetic moment by spin-down states rather than spin-up states in the considered compound.

Table 2. Magnetic moment contribution due to the sub-orbital of Co and Sb atoms in $CoSb_3$ material for GGA: PBE+U functional.

Atoms	Sub-Orbitals	Up-spin (μ_B/cell)	Down-spin (μ_B/cell)	Net magnetic moment (μ_B/cell)
Co	4s	0.092	-0.068	0.024
	$3p_x=3p_y=3p_z$	0.099	-0.094	0.005
	$3d_{xz}=3d_{xy}=3d_{yz}$	0.621	-1.174	-0.533
	$3d_z^2=3d_x^2$	0.460	-1.177	-0.717
	Total	1.272	-2.513	-1.241
Sb	5s	0.381	-0.281	0.100
	$5p_x=5p_y=5p_z$	0.690	-0.760	-0.070
	$4d_{xz}=4d_{xy}=4d_{yz}$	0.018	-0.022	-0.004
	$4d_z^2=4d_x^2$	0.037	-0.040	-0.003
	Total	1.126	-1.103	0.023
$CoSb_3$	Net magnetic moment			-1.218

Conclusions

In the present work, we explored the physical properties of $CoSb_3$ skutterudite material using DFT method of calculations for GGA: PBE+U functional through a VASP computational software. The optimized lattice parameters are found to be fairly in agreement with previous theoretical and experimental reports. The dynamical stability of the material was examined through phonon dispersion calculations, which show no imaginary frequencies, confirming the dynamical stability of the structure. A sharp optical band gap is observed in the higher-frequency region, arising from the rattling vibrations of Co atoms localized within Sb_8 cages. For the prediction of nature of material, we have developed its electronic band structure and density of states (DOS). From the analysis of these plots, we found that $CoSb_3$ skutterudite has metallic properties because electronic band states of atoms are presented around the Fermi energy level. Electrons are spontaneously following from valence band to conduction band in the band structure. For the magnetic properties, we discussed the material's DOS and partial DOS plots and found that asymmetric distributed spin-up and spin-down states around the Fermi energy level and found the magnetic moment of value -1.218 μ_B/cell. This indicates that $CoSb_3$ has magnetic nature. The magnetic moment is obtained due to the dominating value of distributed down-spin states in the orbitals of atoms present in the material. Hence, based on the predicted physical properties of $CoSb_3$ compound, it should be used in the field of spintronic, optoelectronic and electronic device applications.

Authorship Contribution Statement

S. K. Yadhav: Gathering information, analyzing and interpreting it, making figures and graphs, and writing the manuscript.

G. Paudel, A. Devkota & O. S. Rijal: Gathering information, assisting with data analysis and writing the manuscript. Gathering data and contributing to its analysis. H. K. Neupane and R. Parajuli: Developed the idea, oversaw its analysis, interpreted the findings, and thoroughly revised the manuscript.

Acknowledgements

The authors would like to thank the International Science Program (ISP), Uppsala University, Sweden, for supporting the Atmospheric and Material Science Research Group at the Department of physics, Amrit 290 Campus, through NEP01 to conduct the computational work.

Data Availability

The data used to generate the figures and tables are available from the corresponding authors upon request.

Declarations and Conflict of Interest

The authors declare that there is no known conflict of interest.

References

Atkins, P. W., De Paula, J., & Keeler, J. (2023). *Atkins' physical chemistry* (Twelfth edition). Oxford University Press.

Bardeen, J. (1937). On the Density of Energy Levels of Heavy Nuclei. *Physical Review, 51*(10), 799–803. https://doi.org/10.1103/PhysRev.51.799

Caillat, T., Borshchevsky, A., & Fleurial, J. -P. (1996). Properties of single crystalline semiconducting $CoSb_3$. *Journal of Applied Physics, 80*(8), 4442–4449. https://doi.org/10.1063/1.363405

Cococcioni, M., & De Gironcoli, S. (2005). Linear response approach to the calculation of the effective interaction parameters in the LDA+ U method. *Physical Review B—Condensed Matter and Materials Physics, 71*(3), 035105.

Di Ventra, M., & Pantelides, S. T. (2000). Hellmann-Feynman theorem and the definition of forces in quantum time-dependent and transport problems. *Physical Review B, 61*(23), 16207.

Hafner, J. (2008). Ab-initio simulations of materials using VASP: Density-functional theory and beyond. *Journal of Computational Chemistry, 29*(13), 2044–2078.

Hafner, J., & Kresse, G. (1997). The vienna ab-initio simulation program VASP: An efficient and versatile tool for studying the structural, dynamic, and electronic properties of materials. In *Properties of Complex Inorganic Solids* (pp. 69–82). Springer.

Hammerschmidt, L., Schlecht, S., & Paulus, B. (2013). Electronic structure and the ground-state properties of cobalt antimonide skutterudites: Revisited with different theoretical methods. *Physica Status Solidi (a), 210*(1), 131–139. https://doi.org/10.1002/pssa.201228453

Hohenberg, P., & Kohn, W. (1964). Density functional theory (DFT). *Phys. Rev, 136*(1964), B864.

Khan, B., Aliabad, H. A. R., Saifullah, Jalali-Asadabadi, S., Khan, I., & Ahmad, I. (2015). Electronic band structures of binary skutterudites. *Journal of Alloys and Compounds, 647*, 364–369. https://doi.org/10.1016/j.jallcom.2015.06.018

Kohn, W., & Sham, L. J. (1965). Self-consistent equations include exchange and correlation effects. *Physical Review, 140*(4A), A1133.

Kong, L. T. (2011). Phonon dispersion is measured directly from molecular dynamics simulations. *Computer Physics Communications,182*(10),2201–2207. https://doi.org/10.1016/j.cpc.2011.04.019

Li, G., Aydemir, U., Wood, M., Goddard, W. A. I., Zhai, P., Zhang, Q., & Snyder, G. J. (2017). Defect-Controlled Electronic Structure and Phase Stability in Thermoelectric Skutterudite $CoSb_3$. *Chemistry of Materials, 29*(9), 3999–4007. https://doi.org/10.1021/acs.chemmater.7b00559

Li, W., & Mingo, N. (2014). Lattice dynamics and thermal conductivity of skutterudites $CoSb_3$ and $IrSb_3$ from first principles:

Why $IrSb_3$ is a better thermal conductor than $CoSb_3$. *Physical Review B, 90*(9), 094302. https://doi.org/10.1103/PhysRevB.90.094302

Lue, C. S., Lin, Y. T., & Kuo, C. N. (2007). NMR investigation of the skutterudite compound $CoSb_3$. *Physical Review B, 75*(7), 075113. https://doi.org/10.1103/PhysRevB.75.075113

Malki, S., El Farh, L., Challioui, A., & Zanouni, M. (2022). A first-principles investigation on electronic structure and optical properties of tetragonal iron antimonide $FeSb_2$. *Journal of Superconductivity and Novel Magnetism, 35*(6), 1507–1516.

Monkhorst, H. J., & Pack, J. D. (1976). Special points for Brillouin-zone integrations. *Physical Review B, 13*(12), 5188.

Neupane, H. K., Oli, D., Rijal, O. S., Neupane, R. K., Shrestha, P., Sharma, S., Joshi, L. P., & Parajuli, R. (2025). Exploring the structural, dynamical, mechanical, electronic, magnetic, and optical properties of Ta_2AlN, Ti_2AlN & Ti_2GaN MAX phase compounds: First-principles study. *Heliyon, 11*(6), e42962. https://doi.org/10.1016/j.heliyon.2025.e42962

Neupane, H. K., Rijal, O. S., Neupane, R. K., Paudel, G., Shrestha, P., Sharma, S., Joshi, L. P., & Parajuli, R. (2025). Structural, dynamical, thermomechanical, electronic, magnetic, and optical properties of M_2AC (M= Ta, Sc; A= Al, Cd) MAX phase compound Via DFT approach. *Physica Scripta, 100*(9), 095921.

Park, C. H., & Kim, Y. S. (2010). Ab initio study of native point-defects in $CoSb_3$: Understanding off-stoichiometric doping properties. *Physical Review B, 81*(8), 085206. https://doi.org/10.1103/PhysRevB.81.085206

Paudel, G., Nepal, M., Aryal, S., Devkota, A., & Neupane, H. K. (2023). Effect of Water Adsorption on Bilayer h-BN: First-Principles Study. *Journal of Nepal Physical Society, 9*(2), 56–62. https://doi.org/10.3126/jnphyssoc.v9i2.62323

Pokharel, A., Khanal, K., Yadav, S. K., Neupane, T., Paudel, G., Rijal, O. S., & Neupane, H. K. (2025). Exploring the Structural, Electronic, and Magnetic Properties of $MoTe_2$ and $MoSe_2$ Materials Via DFT+U Approach. *Journal of Nepal Chemical Society, 45*(2), 11–24. https://doi.org/10.3126/jncs.v45i2.82919

Rana, B., & Barman, A. (2013). Magneto-optical measurements of collective spin dynamics of two-dimensional arrays of ferromagnetic nanoelements. *3*(01), 1330001.

Rijal, O. S., Neupane, H. K., Oli, D., Neupane, R. K., Shrestha, P., Sharma, S., Joshi, L. P., & Parajuli, R. (2025). A first-principles investigation of the structural, mechanical, dynamic, electronic, magnetic, and optical properties of Ti_2AC (A= Cd, S) MAX phase compounds. *Journal of Physics D: Applied Physics, 58*(12), 125102.

Rodrigues, J. E. F. S., Gainza, J., Serrano-Sánchez, F., Marini, C., Huttel, Y., Nemes, N. M., Martínez, J. L., & Alonso, J. A. (2022). Atomic Structure and Lattice Dynamics of $CoSb_3$ Skutterudite-Based Thermoelectric. *Chemistry of Materials, 34*(3), 1213–1224. https://doi.org/10.1021/acs.chemmater.1c03747

Rogl, G., & Rogl, P. (2019). Skutterudites: Progress and Challenges. In S. Skipidarov & M. Nikitin (Eds.), *Novel Thermoelectric Materials and Device Design Concepts* (pp. 177–201). Springer International Publishing. https://doi.org/10.1007/978-3-030-12057-3_9

Savchuk, V., Boulouz, A., Chakraborty, S., Schumann, J., & Vinzelberg, H. (2002). Transport and structural properties of binary skutterudite $CoSb_3$ thin films grown by dc magnetron sputtering technique. *Journal of Applied Physics, 92*(9), 5319–5326. https://doi.org/10.1063/1.1513188

Togo, A., & Tanaka, I. (2015). First principles phonon calculations in materials science. Scripta Materialia, 108, 1–5. Transport and structural properties of binary skutterudite $CoSb_3$ thin films grown by dc magnetron sputtering technique. *Journal of Applied Physics*. AIP Publishing. (n.d.). Retrieved October 30, 2025, fromhttps://pubs.aip.org/aip/jap/article abstract /92/9/5319/759777/Transport-and-structural-properties-of-binary

Verma, P., & Truhlar, D. G. (2016). Does DFT+ U mimic hybrid density functionals? *Theoretical Chemistry Accounts, 135*(8), 182.

Yadav, S. K., Neupane, T., Pokharel, A., Khanal, K., Deuba, K., Rijal, O. S., & Neupane, H. K. (2025). Exploring the structural, mechanical, dynamical, thermal, electronic, magnetic, and optical properties of monolayer WTe_2 compound: First-principles study. *BIBECHANA, 22*(3), 237–247. https://doi.org/10.3126/bibechana.v22i3.76349

Yu, M., Yang, S., Wu, C., & Marom, N. (2020). Machine learning the Hubbard U parameter in DFT+ U using Bayesian optimization. *Npj Computational Materials, 6*(1), 180.